Applied Catalysis B: Environmental 97 (2010) 1–12

Contents lists available at ScienceDirect

Applied Catalysis B: Environmental

journal homepage: www.elsevier.com/locate/apcatb

Review

Recent achievements in direct ethylene glycol fuel cells (DEGFC)

Alexey Serov*, Chan Kwak

Corporate R&D Center, Samsung SDI, Shin-dong 575, Yeongtong-gu, Suwon-si, Gyeonggi-do 443-731, South Korea

ARTICLE INFO

Article history:
Received 12 February 2010
Received in revised form 25 March 2010
Accepted 10 April 2010
Available online 24 April 2010

Keywords:
Ethylene glycol
Fuel cell
Anode
Catalyst

ABSTRACT

In the present review recent achievements in the development of new type of liquid fed fuel cell, specifically ethylene glycol (EG) operated in acid and alkaline media were summarized. The mechanism of EG electrooxidation in acid media on the platinum surface as well as on different platinum alloys is described. The development in the preparation of new effective electrocatalysts both for ethylene glycol oxidation and oxygen reduction in the presence of EG is discussed. Methods for improving the performance of direct ethylene glycol fuel cells (DEGFC), e.g., MEAs fabrication, operation conditions, etc. are shown.

Contents

1. Introduction

The problem of global climate change caused by greenhouse gases and environmental pollution has forced researchers and manufacturers to search for alternative sources of energy. Among the existing options, including solar power, wind power, tidal power and geothermal power, fuel cells are the most promising source of renewable and clean energy.

Currently, the fuel cells closest to commercial availability are based on direct liquid feeding principles. Fuel cells such as direct methanol fuel cells (DMFC) [1–11], direct ethanol fuel cells (DEFC) [12–22] and direct dimethyl ether fuel cells (DDEFC) [23–36] use liquid fuel and operate at ambient temperatures. These fuel cells have been widely investigated not only by academic researchers but also in several commercial corporations. Analysis of the current stage of research in this field reveals that DMFCs are ready to reach the marketplace, while the FCs using ethanol and DME still need improvements to match the strict specifications in power output, durability and cost. Even though they are the most well-developed direct liquid fed fuel cells, DMFCs still have a number of significant drawbacks. One drawback is dealing with the high price of the final devices. The main contributor to the high cost is the use of platinum and platinum alloys at both sides of the MEAs. This problem can be solved by using alternatives to platinum electrocatalysts. Non-platinum anodes [37] for methanol oxidation as well as cathodes [38–42] for oxygen reduction have been extensively studied in the past few decades, resulting in significant improvements in their catalytic activity. The second problem is the high toxicity of methanol, which can be solved only by strict safety reg-

* Corresponding author. Present address: Paul Scherrer Institute, 5232 Villigen PSI, Switzerland. Tel.: +41 56 5345251; fax: +41 56 3104435.
E-mail addresses: alexey.serov@psi.ch, vores@mail.ru (A. Serov), kcpmhkj@yahoo.com (C. Kwak).

0926-3373/$ – see front matter © 2010 Elsevier B.V. All rights reserved.
doi:10.1016/j.apcatb.2010.04.011

ulations for methanol container design. The third drawback is the methanol crossover from the anode side to cathode. The replacement of the platinum catalyst of the cathode by a non-platinum methanol-resistant catalyst will effectively solve this problem.

During the last few years, several research groups have published their achievements in developing a new type of fuel cell that uses ethylene glycol (EG) as the liquid fuel [43–62]. A significant contribution to the understanding of the mechanism of EG oxidation was the evaluation of different catalysts, and the development of MEAs based on a new type of membrane was performed in the scientific group of Peled and co-workers [43,47,49,52,53,55]. Ethylene glycol has a number of advantages that make it superior to methanol for fuel cell applications. EG has a theoretical capacity 17% higher than that of methanol in terms of Ah ml^{-1} (4.8 and 4, respectively). The boiling point of ethylene glycol (bp 198 °C) is higher than that of methanol (bp 64.7 °C), which makes it safer to work with. Because ethylene glycol is widely used in the automobile industry, the supply chain is already established, which is not true for methanol. All these benefits make fuel cells based on EG a promising source of alternative energy. However, it should be mentioned, that in direct liquid fed fuel cells the fuel should be oxidized completely (or close to 100%), what is still challenging task for DEGFCs. This issue is making the development of new catalysts for complete ethylene glycol oxidation extremely important.

The present review summarizes the recent achievements in addressing the critical issues for successful commercialization of DEGFCs, including optimization of the operating conditions of DEGFCs and screening to determine the optimal choices of catalyst for EG oxidation, membrane type, etc.

2. Mechanism of EG oxidation on the platinum surface

It has been shown that ethylene glycol can be oxidized on the surface of platinum in acidic media, which makes it suitable for application in conventional fuel cells with proton-exchange membranes (Nafion or other types) [63]. The complete oxidation to CO_2 produces $10e^-$ per glycol molecule and can be written as:

$$(CH_2OH)_2 + 2H_2O \rightarrow 2CO_2 + 10H^+ + 10e^- \quad (1)$$

However further investigations resulted in the conclusion that most of the EG is only partially oxidized, producing a number of C_2 intermediates including glycolaldehyde, glyoxal, glycolic acid, glyoxylic acid and oxalic acid [64–68]. At room temperature, the yield of oxidation of ethylene glycol directly to CO_2 is negligible and does not exceed several percent [69].

The general oxidation scheme of EG to intermediate products can be written as [70]:

$$(CH_2\text{–}OH)_2 \rightarrow OH\text{–}C\text{–}CH_2\text{–}OH \quad (2)$$

$$HO\text{–}C\text{–}CH_2\text{–}OH \rightarrow OH\text{–}C\text{–}C\text{–}HO \quad (3.1)$$

$$HO\text{–}C\text{–}CH_2\text{–}OH \rightarrow HOO\text{–}C\text{–}CH_2\text{–}OH \quad (3.2)$$

$$OH\text{–}C\text{–}C\text{–}HO \rightarrow OH\text{–}C\text{–}C\text{–}OOH \quad (4.1)$$

$$HOO\text{–}C\text{–}CH_2\text{–}OH \rightarrow OH\text{–}C\text{–}C\text{–}OOH \quad (4.2)$$

$$OH\text{–}C\text{–}C\text{–}OOH \rightarrow HOO\text{–}C\text{–}C\text{–}OOH \quad (5)$$

Recently, a detailed investigation of the adsorption and oxidation of ethylene glycol and its incomplete C_2 oxidation products glycolaldehyde, glyoxal, glycolic acid, glyoxylic acid and oxalic acid on carbon-supported Pt catalysts was performed by on-line differential electrochemical mass spectrometry (DEMS) under continuous electrolyte flow [61]. The authors proposed that the mechanism of "desorption–re-adsorption–further oxidation" plays an important role during the consecutive oxidation reactions of EG and its derivatives (Fig. 1). This series of experiments gives information about the adsorption and oxidation behavior of ethylene glycol and the products of its partial oxidation on the surface of carbon-supported platinum catalysts in acidic media at room temperature. These results can be summarized as follows. The intermediates with carbonyl groups (aldehydes) interact most strongly with Pt surface, and C–C bond breaking is facile, leading to fast decomposition to CO_{ads}. The interaction between Pt and hydroxyl groups (alcohols) is much weaker than the interaction with carbonyls; therefore, the dissociation rate is low. The adsorption becomes more facile with increasing potential and reaches a maximum of saturation coverage of ~0.6 $\theta_{CO,sat}$. This value is lower than that for adsorption of molecules with carbonyl groups ($\theta_{CO,sat} \sim 0.7$–0.8), which means that further dissociative adsorption is blocked by CO_{ads} at higher CO_{ads} coverages. The carboxyl groups show a weak interaction with the platinum surface, and no C–C bond breakage can be detected in the range of potentials between ~0.1 and 0.95 V. The authors also mentioned that at the relevant potential (<0.7 V), the tendency of these molecules to undergo complete oxidation to CO_2 is rather low. The current efficiencies for CO_2 formation are 6% for EG, ca. 14% for glycolaldehyde, glyoxal and glycolic acid, and about 35% for glyoxylic acid [61]. Oxalic acid can be 100% oxidized to CO_2 only at potentials >0.95 V. The produced intermediates and CO_{ads} compete for active sites of the platinum catalyst preventing the adsorption of new molecules of EG, thereby significantly decreasing the fuel cell performance.

The performed research clearly shows that using EG as a fuel for DEGFCs operated with Pt catalysts at the anode side at ambient temperature will lead to poor fuel utilization and emission of significant amounts of poisonous products of incomplete oxidation. Several approaches can be suggested to increase the performance and eliminate the undesirable emissions. Increasing the platinum loading on the carbon support will increase the probability of re-adsorption of the intermediates, leading to more complete oxidation. The second solution is using platinum alloys with other metals, e.g., Ru, Sn or others. These bi/tri-metallic systems are very efficient for complete oxidation of simple alcohols (methanol) and are widely used in DMFCs. The mechanisms of EG oxidation by such Pt–M catalysts will be discussed later in this review.

3. Development of catalysts for DEGFC

3.1. Anode catalysts for electrooxidation of EG

Currently, the most active catalysts for direct alcohol fuel cells are based on platinum or platinum alloys. The synthesis of these catalysts is well established and allows control of the alloy level, metal ratio and particle morphology. Catalytic electrooxidation of ethylene glycol in acidic media has been mostly studied on platinum and platinum alloy catalysts, including PtRu [43,44,46,50,54,59], PtRuW, PtRuNi, PtRuPd [50], PtSn and PtSnNi [46,48] in supported or unsupported forms.

The influence of the Pt:Ru ratio on the catalytic activity of PtRu/C was studied by Vielstich and et al. [44]. Catalysts were prepared by electrodeposition of the alloy from solutions of H_2PtCl_6 and $RuCl_3$ on gold substrates with Pt:Ru ratios ranging from 92:8 up to 62:38. It was impossible to achieve a higher ruthenium content by this method. The comparison of the catalytic activity for all prepared electrodes was performed by normalizing the measured currents using an "effective" electrode area. The effective electrode area was established by measuring the charge for the oxidation of a CO monolayer. In situ FTIR spectroscopy was used to monitor the reaction products and the influence of the Pt:Ru composition on the reaction pathways. Fig. 2a shows the current–potential curves for EG oxidation for Pt/C and PtRu/C. It is clear that addition of

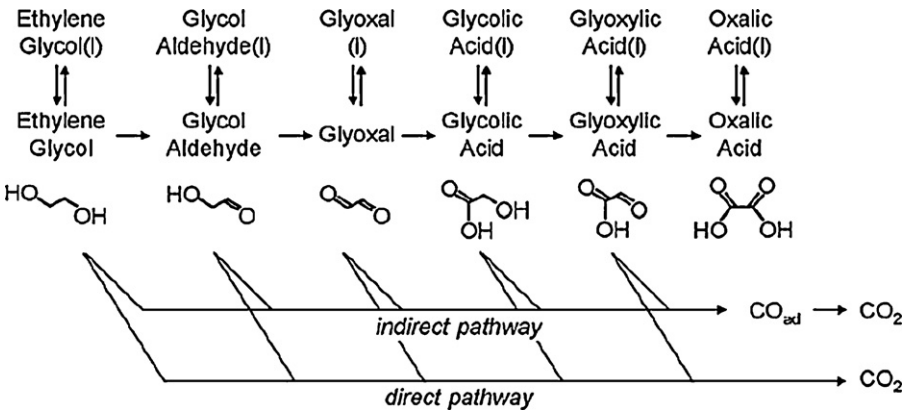

Fig. 1. Reaction scheme for the electrooxidation of ethylene glycol. For reaction in acidic electrolyte at room temperatures and potentials below 0.9 V, the reaction stops at the stage of oxalic acid, which cannot be oxidized under these conditions. Desorption, re-adsorption and further oxidation of the reactive C_2 intermediates increase the formation of higher oxidized reaction products with increasing space velocity.
Reproduced from [61] with permission from Elsevier.

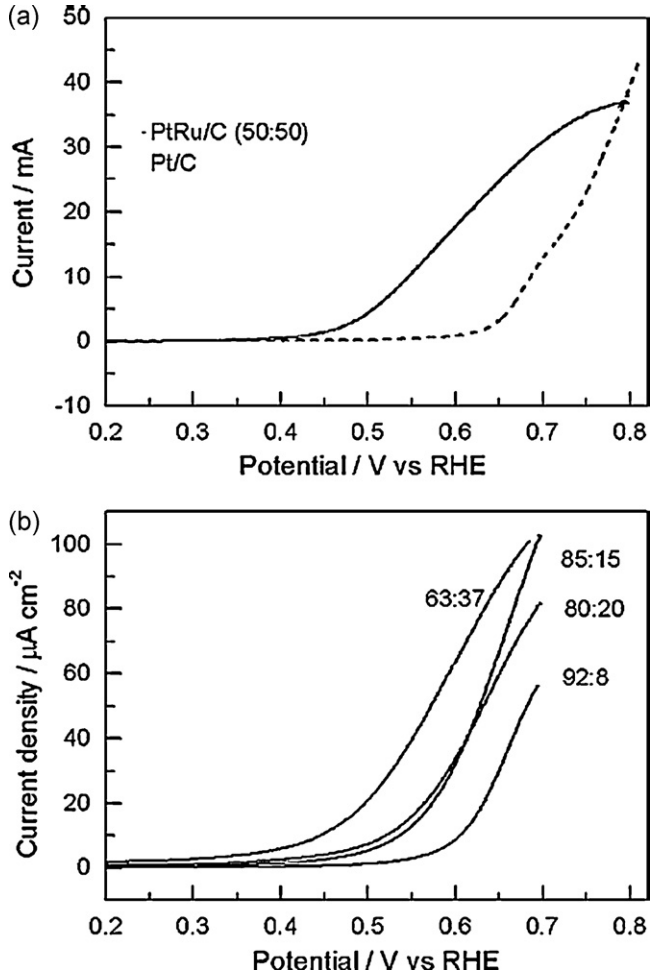

Fig. 2. Current–potential curves for ethylene glycol oxidation at 25 °C. (a) 20% Pt:Ru (50:50)/C and 20% Pt/C in 1 M EG + 0.5 M H_2SO_4; sweep rate 0.5 mV s^{-1}. (b) PtRu electrodeposits on gold; 1 M EG + 0.1 M $HClO_4$; sweep rate 10 mV s^{-1}. The current density is related to the true surface of the active material.
Reproduced from [44] with permission from Elsevier.

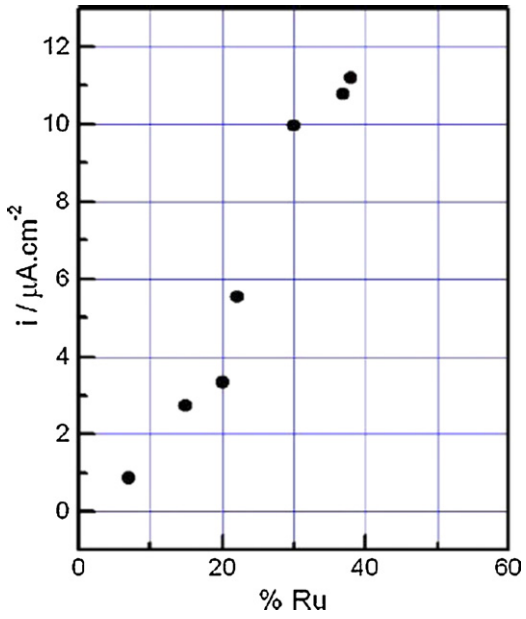

Fig. 3. Current densities for EG oxidation at 0.5 V vs. RHE after 1 h of load for different electrodeposits, plotted vs. the ruthenium content of the catalyst.
Reproduced from [44] with permission from Elsevier.

ruthenium significantly promotes the oxidation reaction. The effect of different Ru concentrations on the electrooxidation of ethylene glycol is shown in Fig. 2b. The current increases with increasing ruthenium content. Additionally, the determination of the optimal Pt:Ru ratio is necessary for designing the best performing catalysts.

The values of the current density after 1 h of load for different PtRu catalysts can be a measure for their catalytic activities (Fig. 3). The current for EG oxidation increases linearly with increasing Ru concentration up to 40% Ru. The authors noted that this behavior differs from that of methanol oxidation at Pt–Ru alloys, where the catalytic activity rapidly increases before reaching a broad maximum at Ru concentrations between 15 and 45% [71]. Based on the data that pure ruthenium does not oxidize ethylene glycol at room temperature, it was suggested that the data in Fig. 3 exhibit a maximum for the promoting effect at some Ru percentage above 40%. Additional experiments on Pt–Ru alloys would be helpful to clarify this point, especially taking into account the fact that one of the most frequently used catalysts for methanol oxidation is Pt:Ru = 50:50. In situ FTIR spectroscopy reveals that besides CO_2, several other intermediates of EG oxidation can be detected (glycolic and/or oxalic acids). Unexpected results were obtained when experiments were performed to evaluate the dependence of the yield of CO_2 on Ru concentration. It was found that the yield of CO_2 decreases with an increase in ruthenium content, which contradicts the data obtained

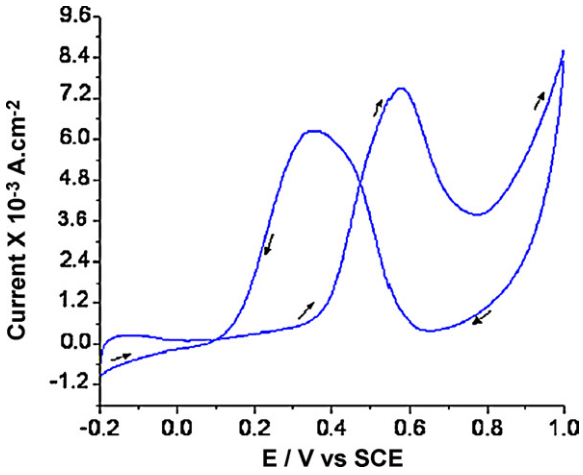

Fig. 4. Electrooxidation of ethylene glycol on Pt nanoparticles modified multi walled carbon nanotubes in 0.5 M H_2SO_4 and 0.5 M EG (scan rate = 50 mV s^{-1}, room temperature).
Reproduced from [54] with permission from Elsevier.

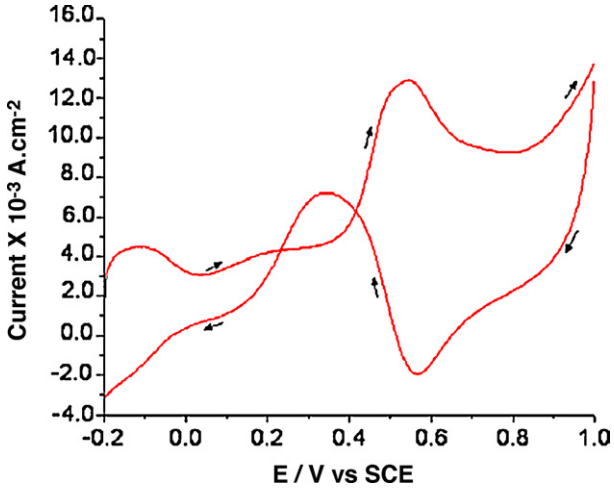

Fig. 5. Electrooxidation of ethylene glycol on Pt–Ru nanoparticles modified multi walled carbon nanotubes in 0.5 M H_2SO_4 and 0.5 M EG (scan rate = 50 mV s^{-1}, room temperature).
Reproduced from [54] with permission from Elsevier.

from the current density experiments (Fig. 3). The authors assumed that the presence of ruthenium catalyses not only the oxidation of adsorbed CO but also parallel pathways, leading to the production of incompletely oxidized intermediates.

Pt and PtRu catalysts deposited on multi walled carbon nanotubes (MWCNTs) have also been studied [54,59]. As can be seen from the cyclic voltammograms (measured at room temperature) of graphite electrodes modified by Pt/CNT (Fig. 4) and PtRu/CNT (Fig. 5), the platinum catalyst modified by ruthenium is more active in ethylene glycol oxidation [54]. Such an enhancement of the catalytic activity can be explained by promotion of CO_{ads} to CO_2 oxidation by the added ruthenium atoms (bi-functional mechanism). The probable mechanism of EG oxidation on bimetallic catalysts can be written as:

$$(CH_2OH)_2 \rightarrow (CH_2OH)_{2(ads)} \quad (6)$$

$$(CH_2OH)_{2(ads)} \rightarrow (:COH)_2 \quad (7)$$

$$(:COH) + 2H_2O \rightarrow (HCOOH)_{ads} + 2H^+ + 2e^- \quad (8)$$

$$Pt(HCOOH)_{ads} \rightarrow Pt(CO)_{ads} + H_2O \quad (9)$$

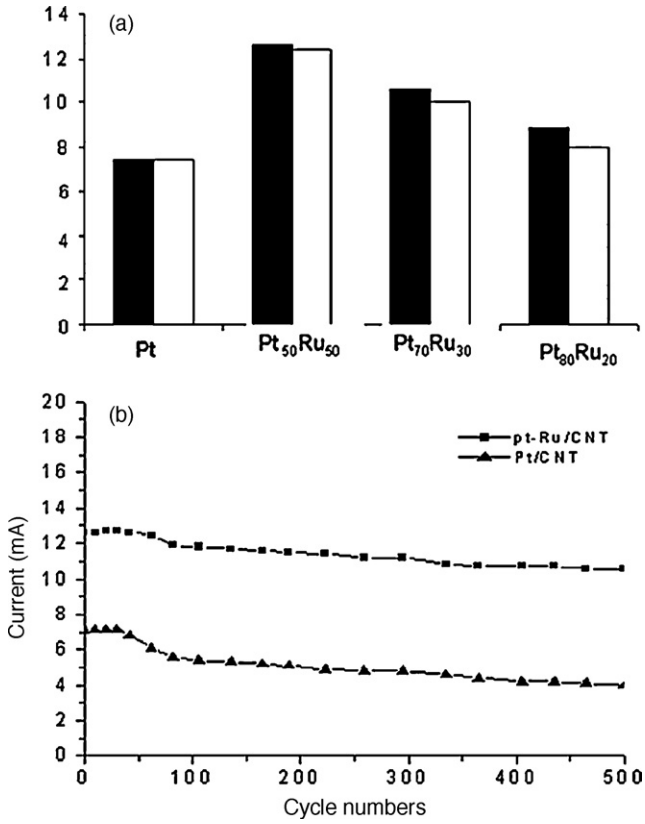

Fig. 6. (a) The effect of Pt/Ru ratio towards EG oxidation. (b) Long term stability of Pt/CNT and Pt–Ru/CNT electrodes in 0.5 M H_2SO_4 and 0.5 M EG (scan rate = 50 mV s^{-1}, room temperature).
Reproduced from [54] with permission from Elsevier.

$$Pt + H_2O \rightarrow Pt(OH)_{ads} \quad (10)$$

$$Pt(OH)_{ads} + Pt(CO)_{ads} \rightarrow Pt + CO_2 + H^+ \quad (11)$$

$$Ru + H_2O \rightarrow Ru(OH)_{ads} + H^+ + e^- \quad (12)$$

$$Ru(OH)_{ads} + Pt(CO)_{ads} \rightarrow Pt + Ru + CO_2 + H^+ + e^- \quad (13)$$

The authors explained the increase of catalytic activity by enhanced ability of added Ru atoms to activate water molecules at a lower potential (0.35 V for Ru compared with 0.6 V for Pt, see Steps 12 and 13). The influence of the Pt:Ru ratio on the catalytic activity in EG oxidation and the long term stability of PtRu/CNT catalysts with different ratios shows that Pt:Ru = 50:50 is the most active and stable catalyst under the studied conditions (Fig. 6). These results are in good agreement with those obtained earlier [44].

A newly designed MEA and the catalytic activity of Pt, PtRu, PtRuW, PtRuNi and PtRuPd deposited on titanium mesh were studied by Chetty and Scott [50]. The authors explained the selection of titanium mesh by noting several features: it is electrochemically stable, electronically conductive and a good support for a diverse range of electrocatalysts [72]. The electrode preparation was based on thermal decomposition of the corresponding salts on the surface of Ti mesh until the desired metal loading was achieved. Fig. 7 shows the scheme of the new MEA compared with the conventional one. The structure of the conventional anode electrode consists of a catalyst layer, a microporous layer and a Teflonized carbon cloth or carbon paper backing layer. In contrast, the mesh-based anode consists of one layer: a titanium mesh coated with catalyst that together is thinner than the conventional electrode. Teflon can be omitted from the mesh anode because it is more hydrophilic than the conventional anode (Fig. 7). Cyclic voltammograms for EG oxidation on the surface of thermally decomposed Pt, PtRu (1:1 ratio)

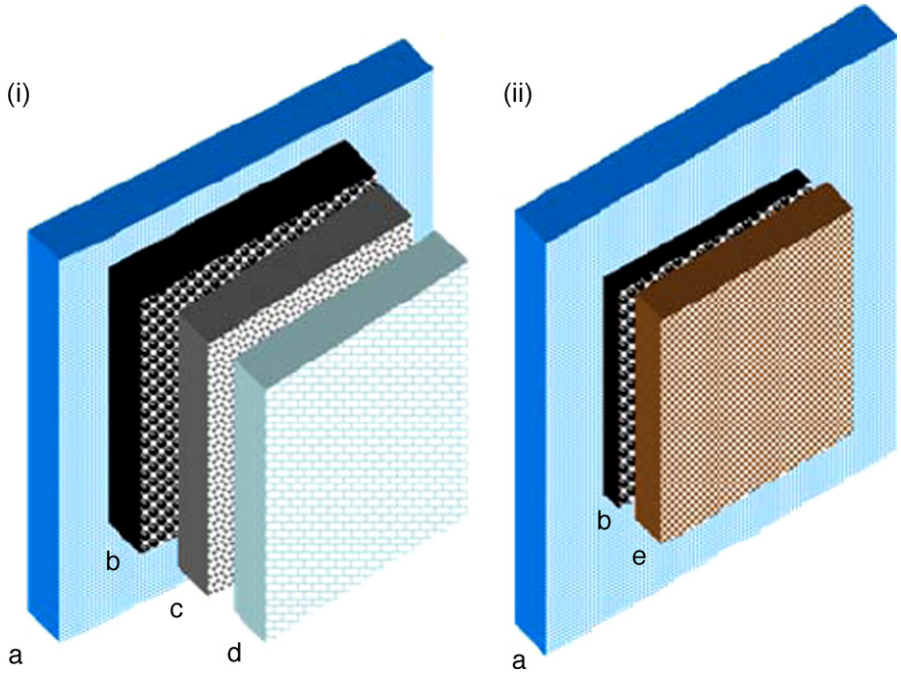

Fig. 7. Schematic representation of (i) conventional anode and (ii) novel mesh-based anode. (a) Polymer electrolyte membrane, (b) catalyst layer, (c) microporous layer, (d) backing layer and (e) titanium mesh.
Reproduced from [50] with permission from Springer.

and PtRuW (1:1:1 ratio) are shown in Fig. 8a, whereas Fig. 8b shows for comparison the voltammogram of Pt/Ti in 0.5 M H_2SO_4. A possible explanation for the broad and poorly resolved peaks is the interaction of Pt with Ti and TiO_x from the mesh [72]. The shapes of the voltammograms for ethylene glycol electrooxidation are similar with those published earlier [73]. Fig. 8a (curves (i) and (ii)) demonstrates the enhanced activity of binary and ternary catalysts (PtRu (1:1 ratio) and PtRuW (1:1:1 ratio)) for ethylene glycol oxidation compared to Pt. The highest activity was achieved for the catalyst with W, which can also be explained by a bi-functional mechanism. In general, the onset potential for alcohol oxidation is attributed to reaction (12). Therefore, it is possible that W lowered the onset potential for ethylene glycol oxidation, especially taking into account the formation of several tungsten oxides (WO_2, W_2O_5, and WO_3). The change in oxidation state of W atoms from W(VI) to W(IV) or from W(VI) to W(V) can render the W sites active for the dissociative adsorption of water [74]. The influence of the addition of Ni and Pd to PtRu on the oxidation of EG was investigated as well. The metal ratio selected was Pt:Ru:M (M = W, Ni, Pd) 1:1:1. The linear sweep voltammograms (LSV) for ethylene glycol oxidation on the surface of the tri-metallic catalysts, obtained at a pseudo-steady state scan rate of 1 mV s^{-1} in the potential range 0–800 mV at 60 °C, are shown in Fig. 9. The catalysts modified by Ni and Pd have no positive effect on the ethylene glycol oxidation, whereas W improves the catalytic activity of PtRu, confirming the abovementioned statements.

A study comparing the activities of new electrocatalysts based on platinum–tin and platinum–tin–nickel alloys with the activity of PtRu was performed by Spinacé et al. [46,48]. PtRu/C and PtSn/C electrocatalysts with Pt:Me atomic ratios between 1:3 and 3:1 were prepared by the alcohol-reduction process [15,16] and tested for ethylene glycol oxidation at room temperature using the thin porous coating technique [75,76]. The performances of PtRu/C and PtSn/C electrocatalysts with different Pt:Ru and Pt:Sn ratio in ethylene glycol oxidation are shown in Fig. 10a and b, respectively. The anodic cyclic voltammetry responses were plotted after subtracting the background currents, and the current values were normalized per gram of platinum, considering that ethylene glycol adsorption and dehydrogenation occur only on platinum sites at ambient temperature. It was found that in the PtRu system, the most active catalyst is Pt:Ru with an atomic ratio of 1:3. This result does not completely agree with previous reports [44,54]. A possible explanation can be offered by taking into account that the XRD data reveal an increase in ruthenium oxide formation with an increase in Ru content. Such ruthenium oxide formation, in analogy to tungsten oxide, can promote the dissociation of water molecules on the Ru surface. In the case of the PtSn alloy, the catalysts with Pt:Sn ratios of 1:1 and 1:3 show better performance than the catalysts with a higher platinum concentration (3:1). The authors explained this behavior by a change in the platinum lattice by the addition of tin, which favors C–C bond breakage. The performance of PtRu/C (Pt:Ru atomic ratio of 1:1 and 1:3), PtSn/C (Pt:Sn atomic ratio of 1:1) and PtSnRu/C (Pt:Sn:Ru atomic ratio of 1:0.5:0.5) electrocatalysts for ethylene glycol electrooxidation is shown in Fig. 11. It can be clearly seen that the PtSn/C 1:1 electrocatalyst shows the best performance in the region of interest for direct alcohol fuel cell applications (0.2–0.6 V) (Fig. 11). Later the same group investigated a PtSn/C electrocatalyst with a Pt:Sn atomic ratio of 50:50 and a PtSnNi/C electrocatalyst with a Pt:Sn:Ni atomic ratio of 50:40:10 [48]. The performance of the PtSn/C and PtSnNi/C electrocatalysts in 1.0 mol L^{-1} of ethylene glycol is shown in Fig. 12. The electrooxidation of ethylene glycol starts at approximately 0.35 V for PtSn/C, while doping of the PtSn catalyst with nickel decreases the onset potential to approximately 0.30 V and increases the current values in all ranges of the potential. The promoting effect of nickel can be explained by modification of the electronic properties of platinum and by the presence of nickel oxide species resulting in a combination of electronic effects and a bi-functional mechanism.

Recently, Jin et al. investigated the electrooxidation of EG on a PtAu catalyst in alkaline, basic and acidic media [56]. It was shown that the highest activity can be achieved in alkaline media. It was also found that the long term stability of PtAu in acidic solution is lower compared with PtRu/CNT.

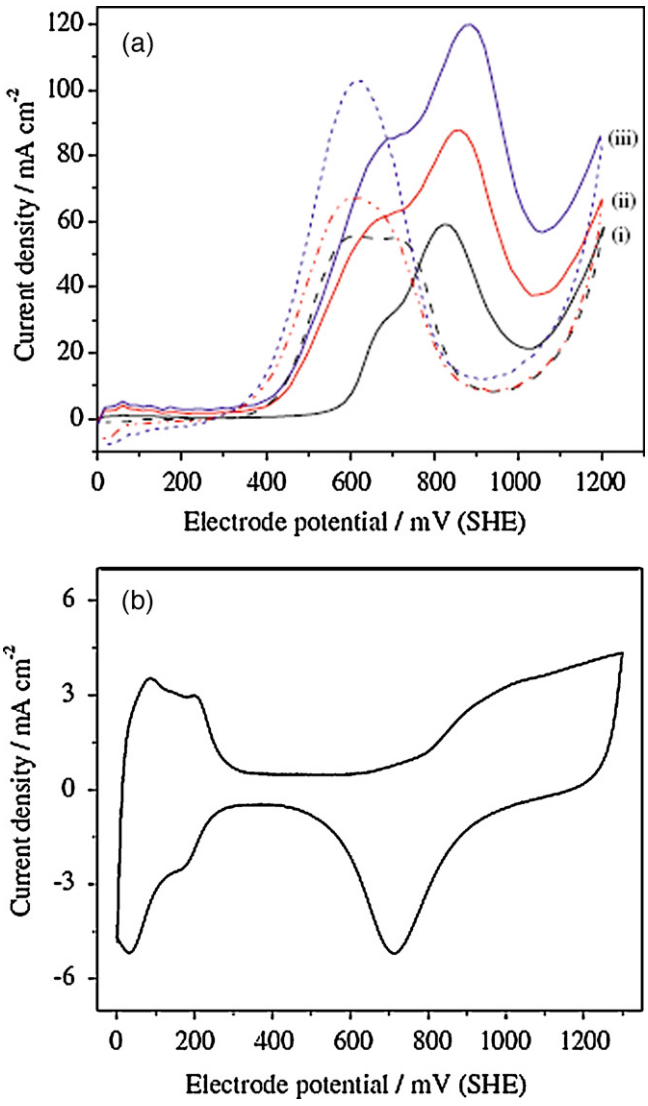

Fig. 8. (a) Cyclic voltammograms for oxidation of 1.0 M ethylene glycol in 0.5 M H_2SO_4 at 20 mV s^{-1} scan rate and room temperature. Thermally decomposed (i) Pt//Ti, (ii) PtRu/Ti and (iii) PtRuW/Ti electrodes. Forward scan (solid line) and reverse scan (dotted line). (b) Cyclic voltammogram of Pt/Ti in 0.5 M H_2SO_4.
Reproduced from [50] with permission from Springer.

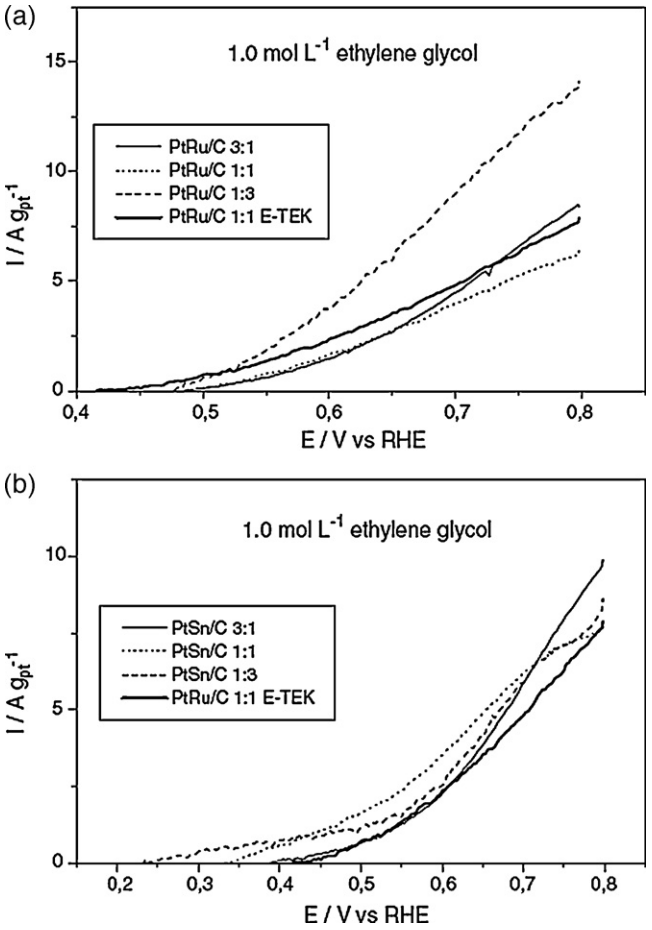

Fig. 10. Cyclic voltammetry of (a) PtRu/C and (b) PtSn/C electrocatalysts in 0.5 mol L^{-1} H_2SO_4 containing 1.0 mol L^{-1} of ethylene glycol with a sweep rate of 10 mV s^{-1}, considering only the anodic sweep.
Reproduced from [46] with permission from Springer.

Considering the facts described above, further research in the field of anode catalysts for EG oxidation is needed. The presence of a second metal in the platinum alloy with the ability to activate water molecules at lower potentials than for Pt significantly increases the catalytic activity. Thus, the systematic screening of Pt–M, where M

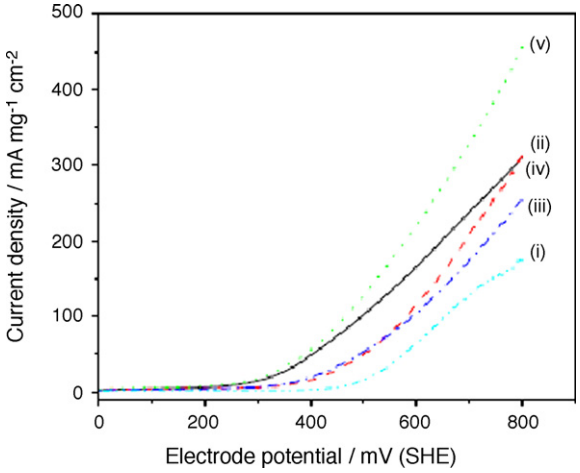

Fig. 9. Linear sweep voltammograms for oxidation of 1.0 M ethylene glycol in 0.5 M H_2SO_4 at 1 mV s^{-1} scan rate at 60 °C on thermally decomposed titanium mesh electrode. (i) Pt, (ii) PtRu (iii) PtRuPd, (iv) PtRuNi and (v) PtRuW.
Reproduced from [50] with permission from Springer.

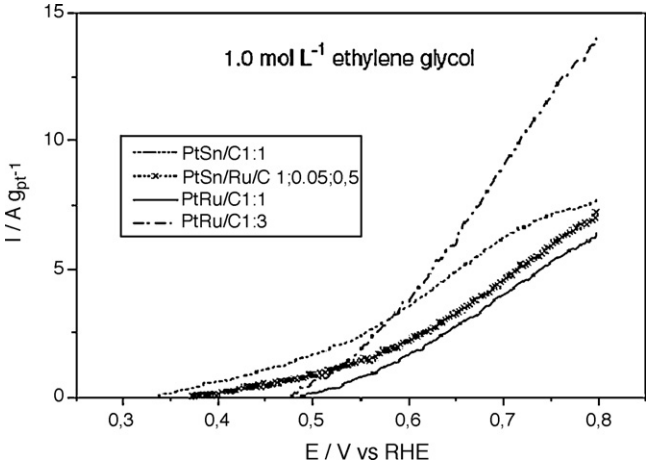

Fig. 11. Cyclic voltammetry of PtSn/C 1:1, PtSnRu/C 1:0.5:0.5, PtRu/C 1:1 and PtRu/C 1:3 electrocatalysts in 0.5 mol L^{-1} H_2SO_4 containing 1.0 mol L^{-1} of ethylene glycol with a sweep rate of 10 mV s^{-1}, considering only the anodic sweep.
Reproduced from [46] with permission from Springer.

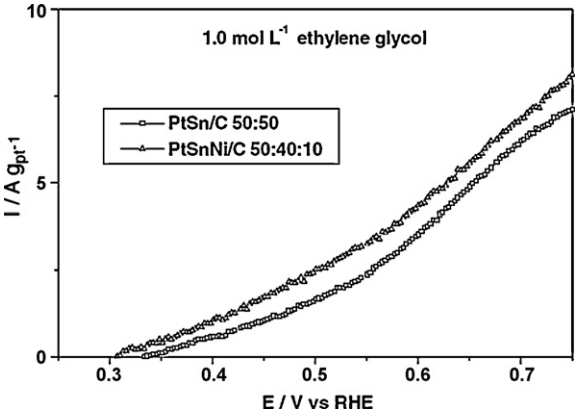

Fig. 12. CV of PtSn/C and PtSnNi/C electrocatalysts in 0.5 mol L^{-1} H_2SO_4, containing 1.0 mol L^{-1} of ethylene glycol with a sweep rate of 10 mV s^{-1}, considering only the anodic sweep.
Reproduced from [48] with permission from Springer.

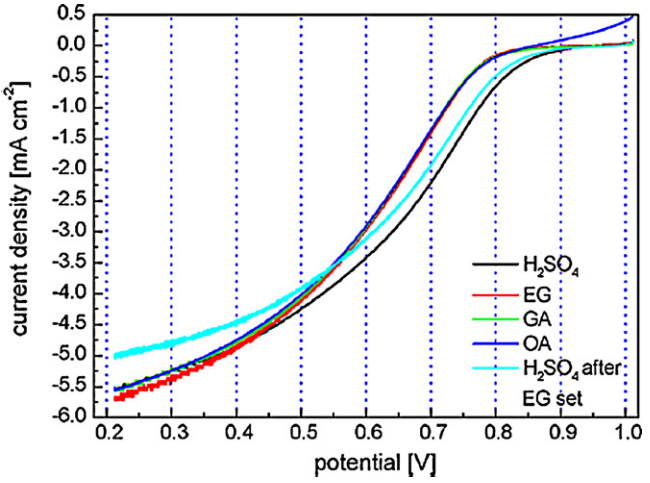

Fig. 13. RDE measured ORR mass activity of commercial Pt 20% (w/w)/XC-72 catalyst measured in 0.5 M H_2SO_4, 0.5 M H_2SO_4 + 0.01 M EG, 0.5 M H_2SO_4 + 0.01 M GA and 0.5 M H_2SO_4 + 0.01 M OA.
Reproduced from [55] with permission from Elsevier.

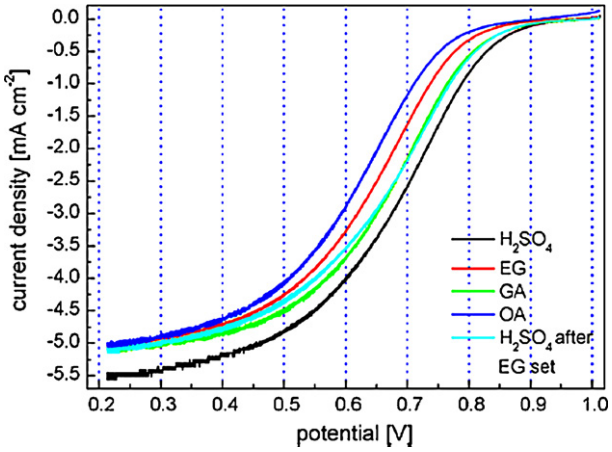

Fig. 14. RDE measured ORR mass activity of homemade PtCoSn 20% (w/w)/XC-72 catalyst measured in 0.5 M H_2SO_4, 0.5 M H_2SO_4 + 0.01 M EG, 0.5 M H_2SO_4 + 0.01 M GA and 0.5 M H_2SO_4 + 0.01 M OA.
Reproduced from [55] with permission from Elsevier.

is a transition or p-block metal, increases the probability of determining the best catalyst for ethylene glycol electrooxidation. In the early stages, the anode catalysts for EG electrooxidation have been developed based on the platinum metals that are optimized for methanol oxidation. However, due to the poisonous intermediates that are generated by ethylene glycol oxidation, different kinds of materials that have both activity in EG oxidation and stability to the poisonous intermediates have to be investigated.

3.2. Cathode catalysts for oxygen reduction in the presence of EG and its derivatives

It has been reported that ethylene glycol and the products of its incomplete oxidation can permeate the cation-exchange membrane and reach the cathode side [44,53]. Up to now, the most frequently used catalyst for the oxygen reduction reaction (ORR) is platinum because of its high activity and stability. However, as was shown above, ethylene glycol and its derivatives exert a strong poisonous effect on the platinum surface. This means that during the ORR, platinum active sites can be partially or completely blocked by by-products of EG oxidation, preventing oxygen reduction and drastically decreasing fuel cell performance. Recently, several articles devoted to the operation of either platinum ORR or Pd-based catalysts in the presence of ethylene glycol and its derivatives were published [55,60,62].

Peled et al. investigated fuel-poisoning tolerant catalysts based on ternary PtCoNi and PtCoSn alloys [55]. The catalysts with total metal loadings of 20 wt.% supported on Vulcan XC-72 (Cabot) were prepared by a classic electroless deposition process with the activation of a carbon-powder surface [77]. As prepared, the electrocatalysts were treated with 1 M H_2SO_4 at 80 °C for 15 h to obtain stable catalysts with platinum-skin structures. To compare the activity of the homemade catalysts with the commercial PtCo/Vulcan XC-72 catalyst (E-TEK, 20 wt.%), the commercial catalyst was also acid-treated. Experiments on fuel poisoning were conducted in the following solutions: 10 mM MeOH, 10 mM formaldehyde, 10 mM formic acid, 10 mM EG, 10 mM glycolic acid (GA) and 10 mM oxalic acid (OA) + 0.5 M H_2SO_4. CV curves of ORR in the presence of EG, GA and OA for the commercial Pt/C and homemade PdCoSn/C catalysts are shown in Figs. 13 and 14, respectively. It was found that ethylene glycol decreased the catalytic activity less than glycolic acid, and oxalic acid was the most poisonous species (Figs. 13 and 14). The authors suggested that the degree of poisoning mainly depends on which species is the hardest to oxidize and therefore the most strongly adsorbed on the catalyst surface. In the EG oxidation reaction mechanism, oxidation of EG to GA through glycolaldehyde is considerably faster than GA oxidation to OA through glyoxylic acid, making OA the hardest intermediate to oxidize [78]. Thus, the oxidation of oxalic acid by-products is slower than oxidation of ethylene glycol, leading to strongly adsorbed species that prevent oxygen adsorption and reduction. The absence of positive currents also supports these suggestions. The authors proposed two possible mechanisms of enhanced cathode tolerances. One mechanism is based on the lower activity of cathode alloy catalysts towards fuel oxidation compared to pure platinum. This would lead to reduced fuel adsorption on their surface, thus decreasing the interference of the oxidation reaction of the fuel with the ORR. The second mechanism deals with higher fuel-oxidation activity, which can also decrease the ORR catalyst poisoning by decreasing the adsorption of the fuel and its by-products on the catalyst surface due to its easier oxidation and removal [79]. The experiments with the bulk oxidation of EG on the surface of Pt/C, PtCo/C and PtCoSn/C reveal that PtCoSn/C has the highest onset potential among all the catalysts. This result is in agreement with its higher tolerance towards ORR fuel poisoning due to its lower fuel-oxidation activity, thus supporting the first hypothesis.

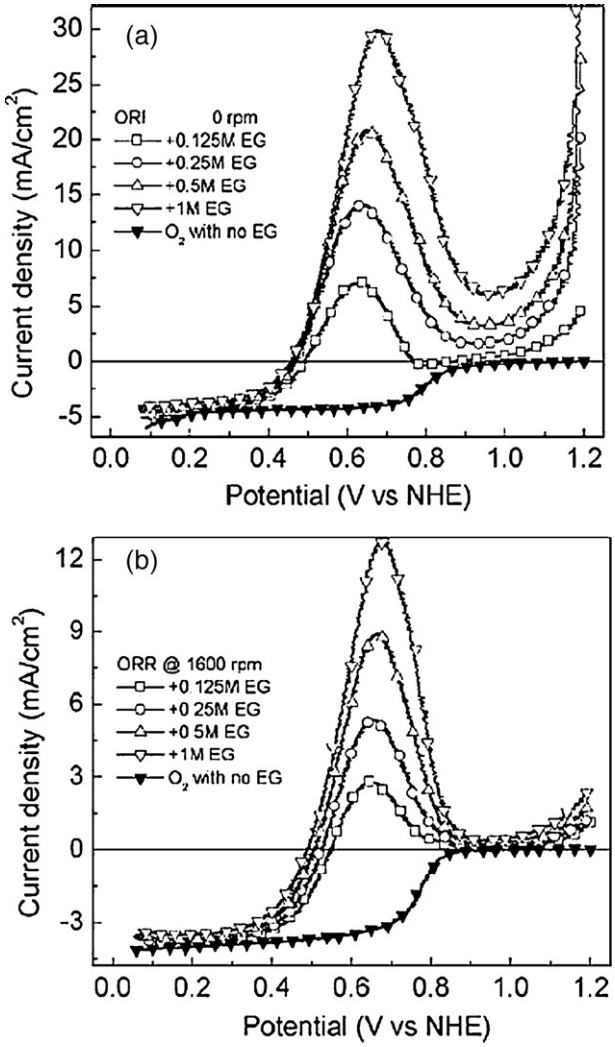

Fig. 15. LSVs of the ORR without and with EG at (a) Pt/C (b) Pt/CNT. Reproduced from [62] with permission from Elsevier.

The behavior of carbon-supported Pd-only (20 wt.% E-Tek) electrocatalysts for the ORR in the presence of EG was studied by Rodríguez Varela et al. [60]. A standard Pt/C (20 wt.% E-Tek) electrocatalyst was also tested to compare with the performance of Pd/C. LSVs of the ORR using the 20 wt.% Pt/C and Pd/C electrocatalysts with several increasing EG concentrations. It was found that the Pd/C catalysts show a high tolerance to EG oxidation. In contrast with Pt/C, the ORR curve does not have any peaks related to ethylene glycol oxidation. Despite the fact that the activity of palladium catalysts in the absence of EG is lower than the activity of platinum, the total performance of the DEGFC can be significantly higher with a Pd/C cathode catalyst.

Later, the same group investigated the tolerance of $Pt_{40}Pd_{60}$ deposited onto CNTs toward EG oxidation [62]. The polarization curves with and without EG for Pt/C (Fig. 15a) and Pt/CNTs (Fig. 15b) show that the catalyst supported on carbon nanotubes is relatively more resistant to the presence of EG; however, a drastic decrease in ORR performance is observed for both catalysts (Fig. 15a and b). Fig. 16 shows the LSVs at the PtPd/CNT electrocatalyst in the presence of increasing EG concentrations. It was found that the PtPd/CNT catalyst shows a high tolerance to EG oxidation up to an EG concentration of 0.25 M. At higher EG concentrations, current density peaks appeared at Pt–Pd/CNT, although these peaks were significantly less intense than those at Pt/C and Pt/CNT. It can be concluded that because this research did not include a search for

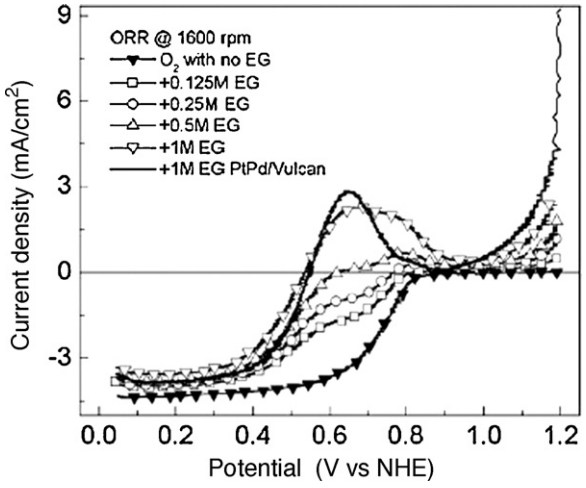

Fig. 16. Polarization curves of the ORR at Pt–Pd/MWCNT with EG. Reproduced from [62] with permission from Elsevier.

the optimal Pt:Pd ratio, the catalytic activity for the ORR and the EG oxidation tolerance could be increased after optimization of the catalyst preparation.

Most of the publications dealing with cathodes tolerant to EG and its derivatives were published in the last year, showing the growing interest in this subject. From our point of view, the search for catalysts that are the most active for the ORR and resistant to oxidation of EG should be started with the evaluation of different non-platinum ORR catalysts. These catalysts, which have already been studied for DMFC applications, include RuSe/C, Pd_xCo_y/C, heat treated macrocycles and others. Some of these catalysts possess activity comparable with the activity of Pt along with high tolerance to MeOH oxidation [42].

4. Membranes, MEAs and DEGFC performance

There have been several articles published about DEGFC performance [43,44,47,50,53]. The studied fuel cells can be separated into two categories: the first uses a commercially available Nafion™ membrane [44,50], and the second uses a new type of nanoporous proton-conducting membrane (NP-PCM) developed by Peled et al. [43,47,53]. The representative commercial Nafion™ is suitable for the hydrogen fuel cells operated below 80 °C. The low reactivity of EG and poisoning of the electrode by toxic intermediates requires a high operating temperature. Accordingly, newly developed membranes should be proven against higher temperatures to be used in direct EG fuel cells.

Vielstich et al. investigated the performance of a DEGFC based on a Nafion™ 117 membrane operated at 70 °C with 2 M EG at the anode and O_2 at the cathode side [44]. A constant anode potential of 0.4 V was applied, and the current response was followed during 1 h of operation. Fig. 17 shows the current–time data. The current density started above 25 mA cm^{-2} and achieved a near stationary value of about 18 mA cm^{-2}. During the experiment, the authors noticed that the crossing over of EG and the products of its incomplete oxidation from the anode to the cathode side exerted a strong influence on fuel cell performance. The significant decrease of the oxygen potential during the first 30 min confirms the poisonous effect of EG, as discussed above.

Scott et al. used an MEA with a modified anode (Fig. 7), a Nafion™ membrane, operated at 90 °C with 1 M EG and O_2. PtRu/C, PtRu/Ti and PtRuW/Ti were used as anode catalysts. The fuel cell polarization curves are shown in Fig. 18. The open circuit voltages are approximately 0.47 V for PtRu/Ti and 0.46 V for PtRu/C. It was

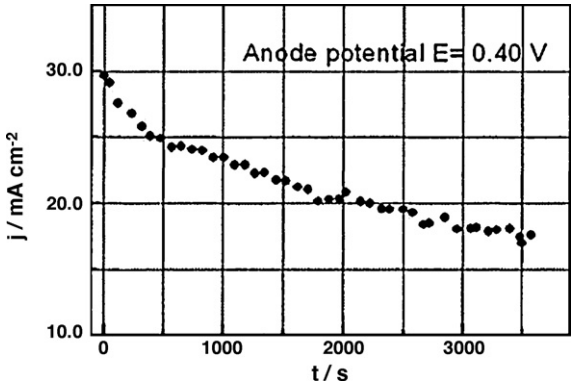

Fig. 17. Current density (related to the geometric area) vs. time at a potential of 0.4 V obtained for the anode of an EG/O_2 fuel cell, using Nafion 117 as polymer electrolyte, 2 M EG, 1 cm^3 min^{-1} liquid flow in the anode chamber, geometric active surface 4.6 cm^2, dry oxygen at 1 atm, 70 °C.
Reproduced from [44] with permission from Elsevier.

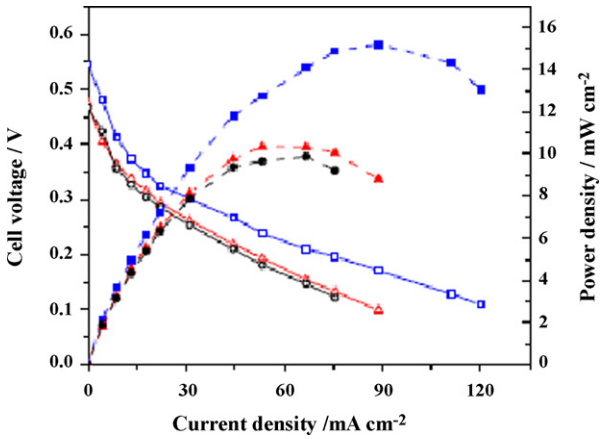

Fig. 18. Fuel cell polarization data for thermally decomposed PtRuW, PtRu and E-Tek PtRu/C anodes measured at 90 °C in 1 M ethylene glycol and 1 bar oxygen. Anode catalyst loading 2 mg cm^{-2} and cathode catalyst 2 mg cm^{-2} of 60 wt.% Pt/C (E-Tek). Current density (open symbol) and power density (full symbol) for PtRu/C (○,●), PtRu/Ti (△,▲) and PtRuW/Ti (□,■) anodes.
Reproduced from [50] with permission from Springer.

found that the maximum power densities are 10 and 9 mW cm^{-2} for the PtRu/Ti and PtRu/C anodes, respectively. The PtRuW/Ti anode gave an open circuit voltage of 0.55 V and a maximum power density of 15 mW cm^{-2}, clearly demonstrating its higher activity for ethylene glycol oxidation.

The second class of DEGFC operated with a new membrane type – nanoporous proton-conducting membrane (NP-PCM) – was extensively studied in the group of Peled [43,47,53]. A nanoporous proton-conducting membrane with a typical pore size of ~1.5 nm consists of ceramic nanopowder, poly(vinylidenedifluoride) (PVDF) and an acid electrolyte [80]. The authors emphasized that the usage of NP-PCM has a number of advantages compared with Nafion™: (1) lower membrane cost (by more than two orders of magnitude); (2) smaller pores (by a factor of two); (3) lower methanol crossover (by up to an order of magnitude), which leads to much higher fuel utilization; (4) higher conductivity (by up to four times); (5) the ionic conductivity of the NP-PCM, unlike Nafion, is not affected by heavy metal impurities; and (6) as the corrosion products of heavy metals do not affect its conductivity, it permits the use of cheaper catalysts and hardware materials [43]. The authors used membrane electrode assembly (MEA) based on a 100- or 240-μm thick nanoporous proton-conducting membrane (NP-PCM) made of PVDF and SiO_2. The anode catalyst was platinum–ruthenium (1:1 atomic ratio) nanopowder (Johnson-Matthey), and the cathode was platinum (both anode and cathode loading was 4 mg cm^{-2}). Oxygen was fed at 1–4 atm (abs) into the cathode compartment through a water bubbler at 65–95 °C at the rate of 40–60 ml min^{-1}. During cell operation, an aqueous solution of 3 M sulfuric acid and a fuel (0.5–2 M methanol or EG) was circulated past the anode at a flow rate of 15 ml min^{-1}. Fig. 19 presents the power density data for a Nafion-based DMFC, an NP-PCM-based DEGFC and an NP-PCM-based DMFC; the values for these cells are 260, 300 and over 400 mW cm^{-2}, respectively [44]. It was observed that neither catalysts nor operation conditions were optimized for obtaining the highest performance for DEGFCs. Further development can result in higher power densities for direct ethylene glycol fuel cells.

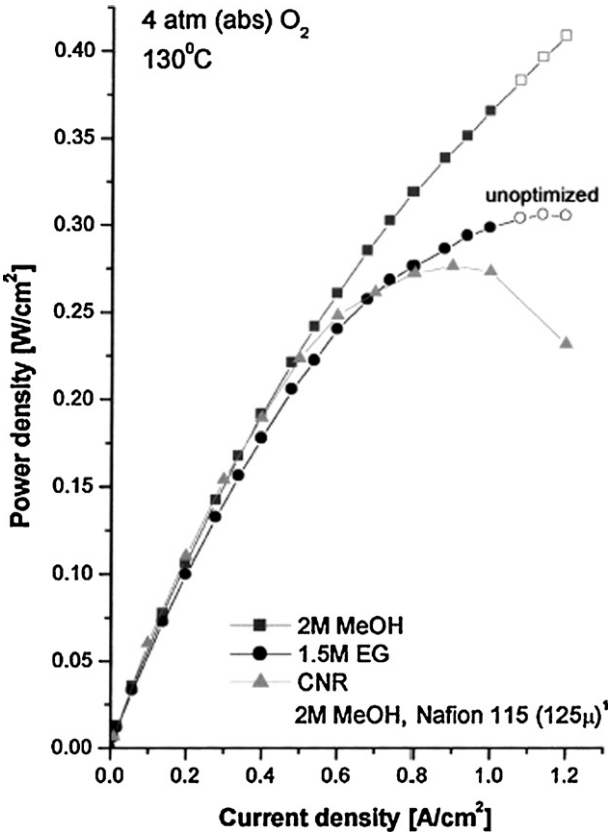

Fig. 19. Power density of DMFC and DEGFC based on 100 μm NP-PCM.
Reproduced from [43] with permission from Elsevier.

Later, Peled and Livshits published new data for a DEGFC (reported earlier [43]) performed at different temperatures and using air instead of oxygen [47]. The composition of the nanoporous proton-conducting membrane (NP-PCM) was 28 wt.% poly(vinylidenedifluoride) (PVDF), 12% SiO_2 and 60% liquid volume (that is, filled with an acid-fuel solution). A solution of 1 M methanol or 0.72 M ethylene glycol and 1.7 M triflic acid or 0.5 M ethylene glycol and 2 M sulfuric acid was fed to the anode, and dry air was supplied to the cathode. Fig. 20 depicts the triflic acid-based DEGFC performance at several temperatures: 65 and 80 °C (at 0.9 atm dry air), 110 and 130 °C (at 3.7 atm dry air). Maximum power densities of 45, 80, 285 and 320 mW cm^{-2}, respectively, have been achieved under these conditions. Raising the operating temperature of the DEGFC from 80 to 110 °C resulted in a significant improvement in the performance of both anode and cathode. The authors explained this improvement by a lower level of poisoning of the Pt catalyst by EG and its oxidized species on the cathode side.

An evaluation of the performance of the DEGFC stacks with analysis of the intermediate oxidation products was performed by

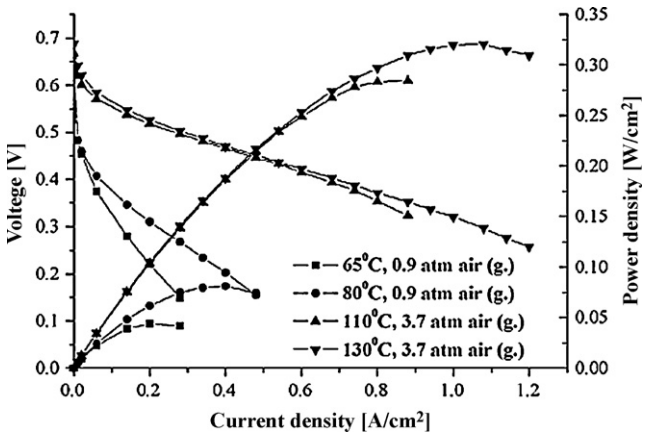

Fig. 20. NP-PCM-based DEGFC performance at 65–130 °C. NP-PCM (85 μm), 0.72 M EG, 1.7 M triflic acid, no air humidification, 4 mg Pt cm^{-2} on each electrode. Reproduced from [47] with permission from Elsevier.

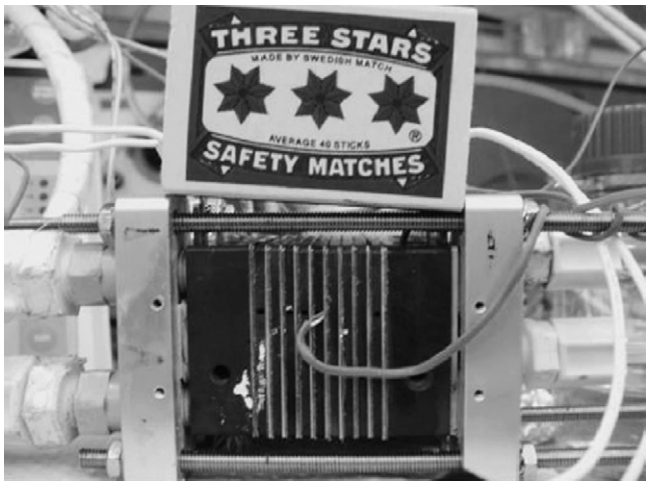

Fig. 21. A 10 (10 cm^2) cell direct ethylene glycol fuel cell (DEGFC) stack. Reproduced from [53] with permission from Elsevier.

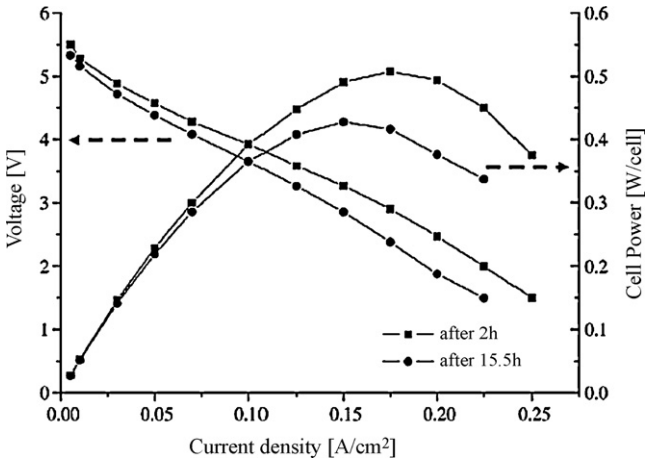

Fig. 22. Stack 2 performance after 2 and 15.5 h of test (triflic acid). Reproduced from [53] with permission from Elsevier.

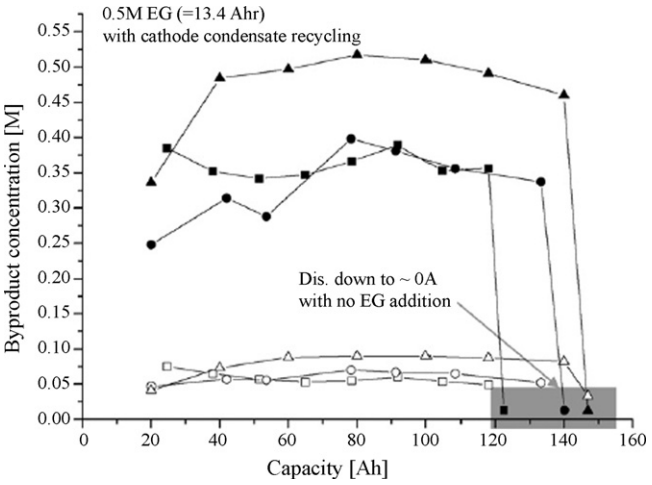

Fig. 23. Time-dependent concentrations of GA and OA in DEGFC stacks. (■) Pt–Ru black (JM), stack 1, 1.7 M triflic acid, GA; (●) BASF Pt–Ru (1:0.7), stack 2, 1.7 M triflic acid, GA; (▲) BASF Pt–Ru (1:0.7), stack 2, 2 M sulfuric acid, GA; (□) Pt–Ru black (JM), stack 1, 1.7 M triflic acid, OA; (○) BASF Pt–Ru (1:0.7), stack 2, 1.7 M triflic acid, OA; (△) BASF Pt–Ru (1:0.7), stack 2, 2 M sulfuric acid, OA. Reproduced from [53] with permission from Elsevier.

Peled et al. [53]. These stacks were constructed from ten 10-cm^2 cells based on 2.2-mm bipolar plates (Fig. 21). The anode catalysts used in the stacks were different: stack 1 utilized PtRu-black catalyst (Johnson-Matthey), while stack 2 was based on supported PtRu (1:0.7 ratio, BASF). A constant volume (100 ml) of fuel solution, 0.5 M ethylene glycol and 1.7 M triflic acid, was circulated in a closed loop over the anode compartments of both stacks. In an additional test, stack 2 was run with a similar fuel solution containing 2 M sulfuric acid (instead of triflic acid), which was circulated in the same manner. The authors found that a concentration of about 0.5 M EG was optimal for these tests. Two to three equivalents of ambient, dry air (room air, not filtered) was fed into the cathode compartments of both stacks [53]. Stacks 1 and 2 were operated for more than 10 fuel turnovers. The operating conditions were very close to the conditions of a conventional fuel cell (T = 80 °C, limited fuel solution volume, recycling of both the fuel solution and the cathode condensate in a closed loop). Stack 2 exhibited very high initial performances of more than 120 mW cm^{-2} (while fed with the triflic acid-fuel solution) and close to 60 mW cm^{-2} (with the sulfuric acid-fuel solution) at 0.3 V $cell^{-1}$. The polarization curves of stack 2 (operating with triflic acid) under steady state conditions exhibit performance drops from 50 to 43 mW cm^{-2} after 2 and 15.5 h of operation (Fig. 22). Such a performance drop of both stacks (regardless of the acid type) can be explained by the formation of EG oxidation by-products (glycolic and oxalic acids) (Fig. 23).

The authors summarized that after 10 fuel turnovers, a continuous discharge without any EG addition was conducted, at the end of which only minor amounts of GA and OA remained in the fuel solution. Together with the data of the electrochemical (potentiostatic) titration, these results demonstrate 94% fuel efficiency for EG [81]. Such high fuel utilization makes fuel cells based on ethylene glycol promising candidates for commercialization.

5. Ethylene glycol fuel cells operated in alkaline media

In the present review, we have paid attention mainly to the development of DEGFCs operated in acidic media (catalysts, MEA, stacks, etc.), due to the fact that all the components of these fuel cells (catalysts stable to acidic media, proton-conductive membranes, corrosion-resistant separators, etc.) are commercially available and can be used in direct ethylene glycol fuel cells. On the other hand, as was shown previously in this review, the mechanism of EG oxidation in acid media is complicated, the kinetics of oxidation are slow and the catalysts performance is still not optimized. These issues have driven researchers to investigate the processes occurring during oxidation of ethylene glycol in alkaline solutions,

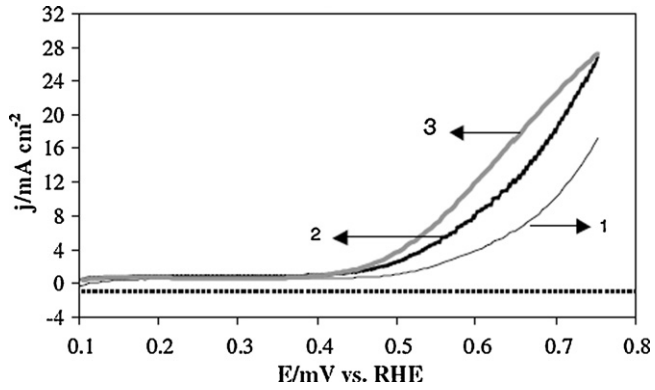

Fig. 24. $j(E)$ Polarization curves of (1) Pt/C, (2) $Pt_{0.9}Bi_{0.1}/C$, (3) $Pt_{0.45}Pd_{0.45}Bi_{0.1}/C$ catalysts recorded in 0.2 M NaOH + 0.1 M EG at $\nu = 50$ mV s^{-1} and 20 °C.
Reproduced from [51] with permission from Elsevier.

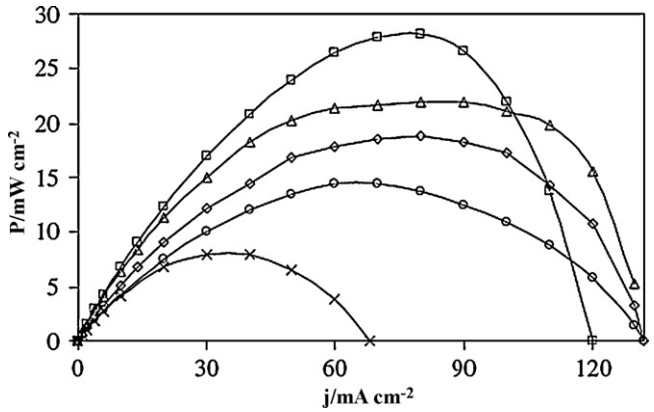

Fig. 25. Power density vs. current density curves recorded at 20 °C for 2 M ethylene glycol with 4 M NaOH. Anodes (◊) Pt/C 40 wt.%, (×) Pt/C 20 wt.%, (○) Pd/C 20 wt.%, (△) $Pt_{0.9}B_{i0.1}/C$ 50 wt.%, (□) $Pt_{0.45}Pd_{0.45}Bi_{0.1}/C$ 50 wt.%. Homemade cathodes are Pt/C 40%. All electrodes were loaded with 2 mg cm^{-2} of catalyst. Anionic membrane is Moragne-ADP from Solvay.
Reproduced from [51] with permission from Elsevier.

perform searches for new active catalysts for operation in alkaline media and study the performance of alkaline DEGFCs [45,51,56,57].

The electrooxidation of EG in alkaline media along with an analysis of the products of oxidation and their poisonous effect was performed by Ogumi et al. [45]. The authors used constant-potential electrolysis at potentials of 400 and 500 mV to obtain information about the formation of products by the oxidation of methanol or ethylene glycol. It was found that electrooxidation of ethylene glycol at 400 mV gave glycolate, oxalate and formate. The concentrations of all products increased in proportion to the applied potential: the current efficiency was 40% for glycolate production, ~15% in the case of formate and about 10% based on oxalate formation [45]. The authors noticed that oxalate is a very stable product in alkaline solution and can be neither further oxidized nor adsorbed on platinum in alkaline solutions, resulting in the formation of non-poisonous substances. The second series of experiments at 500 mV revealed a drastic difference in ethylene glycol oxidation compared to 400 mV. The current efficiency of glycolate (main product at 400 mV) decreased from ca. 40 to 18%, and that of formate increased from ca. 15 to 20%. This difference in behavior can be explained by C–C bond cleavage in ethylene glycol at over 500 mV. Such a C–C bond breakage can lead to formation of CO_{ads} with further poisoning of the platinum catalysts.

The influence of atoms added to platinum catalysts on the electrooxidation of EG in alkaline medium was studied by Léger et al. [51]. The catalysts Pt/C, PtPd/C ($Pt_{0.5}Pd_{0.5}$), PtBi/C (Pt_xBi_{1-x} (with x from 0.9 to 0.7)) and PtPdBi/C ($Pt_{0.45}Pd_{0.45}Bi_{0.1}$) were prepared by the "water-in-oil" method [82]. The authors found that among the tested catalysts, the most active for EG oxidation in alkaline medium were Pt/C 40 wt.%, $Pt_{0.5}Pd_{0.5}/C$ 20 wt.%, $Pt_{0.9}Bi_{0.1}/C$ and $Pt_{0.45}Pd_{0.45}Bi_{0.1}/C$ 50 wt.% (Fig. 24). The difference in optimal metal loading may be explained by a size effect and/or the active surface area. Analysis of the products of EG oxidation performed at a closed fuel circuit shows that after 360 min of product accumulation, glycolic acid, oxalic acid and some traces of formic acid are detected at the Pt/C anode, whereas glycolic acid, oxalic acid and traces of glyoxylic acid are detected with the Bi-containing catalysts. This result confirms that platinum is able to break the C–C bond of EG at ambient temperature in alkaline medium. The catalysts with addition of Bi or PdBi do not form formic acid, which indicates that the dilution of platinum sites leads to a decrease in the ability to break the C–C bond. To carry out the test of DEGFC performance, the authors used an anion-exchange membrane (ADP-Morgane membrane) provided by Solvay, which was made from a cross-linked fluorinated polymer carrying quaternary ammonium ions as exchange groups. Fig. 25 compares the performance obtained with a solid alkaline fuel cell (SAMFC) fitted with different anodes: Pt/C, $Pt_{0.9}$ $Bi_{0.1}/C$ and $Pt_{0.45}Pd_{0.45}Bi_{0.1}/C$. The addition of Bi to platinum leads to an increase in open circuit voltage from 0.66 to 0.83 V. Such an increase of OCV can be explained by the higher activity of the PtBi catalyst towards EG electrooxidation, which leads to a decrease in EG concentration in the vicinity of the membrane and lowers the crossover effect. The MEA with PtBi reached a maximum value of power density of 22 mW cm^{-2}. The best performances under the same experimental conditions were obtained using the PtPdBi/C anode with a maximum achieved power density of 28 mW cm^{-2}, confirming the beneficial effect of the addition of palladium. The enhancement of electroactivity in the presence of bismuth was explained by the authors mainly in terms of the bi-functional theory of electrocatalysis, whereas the benefic effect of palladium was explained mainly in terms of reduction of the poisoning effect [51].

The slow kinetic rate of EG oxidation in the anode can be improved with the help of OH^- groups transferred from the cathode side in the direct EG fuel cell. As in other cases of low anode kinetics, alkaline electrolytes are better than acid electrolytes for the direct EG fuel cell. However, the development of a stable alkaline membrane is crucial for the use of alkaline media.

6. Conclusions

As a promising fuel for direct-fed fuel cells, EG has attracted the attention of many researchers in the world. The number of publications is increasing from year to year, indicating the progress in this field. It was shown in our review that many of the problems preventing the commercialization of direct ethylene glycol fuel cells, such as understanding the mechanism of EG electrooxidation, discovering methods of increasing catalytic activity of platinum based catalysts and development of new membrane types, have already been solved or will be solved soon. However, we should also mention that significant efforts should be applied toward increasing the performance of the final product. This can be achieved by sequential improvement of the performance of each of the FC components. The anode catalysts should be optimized for EG oxidation without being poisoned by its derivatives, whereas the cathode catalysts should show high ORR activity with full tolerance of the oxidation of ethylene glycol and its intermediates. The development of commercial Nafion™ or new types of proton-conducting membranes is also required. Selection of the best performing catalysts, membranes, bipolar plates and other components will result in the production of a highly effective source of green power.

References

[1] K. Scott, W. Taama, J. Cruickshank, J. Power Sources 65 (1997) 159–171.
[2] X. Ren, P. Zelenacy, S. Thomas, J. Davey, S. Gottesfeld, J. Power Sources 86 (2000) 111–116.
[3] A. Heinzel, V.M. Barragan, J. Power Sources 84 (1999) 70–74.
[4] V. Baglio, A.S. Aric'o, A. Di Blasi, V. Antonucci, P.L. Antonucci, S. Licoccia, E.S. Fiory, Electrochim. Acta 50 (2005) 1241–1246.
[5] H. Dohle, J. Divisek, J. Mergel, H.F. Oetjen, C. Zingler, D. Stolten, J. Power Sources 105 (2002) 274–282.
[6] X. Ren, T.E. Springer, T.A. Zawodzinski, S. Gottesfeld, J. Electrochem. Soc. 147 (2) (2000) 466–474.
[7] Z. Jusys, T.J. Schmidt, L. Dubau, K. Lasch, L. Jorissen, J. Garche, R.J. Behm, J. Power Sources 105 (2002) 297–304.
[8] Y. Morimoto, E.B. Yeager, J. Electroanal. Chem. 444 (1998) 95–100.
[9] H. William, L.-V.A. Paganin, E.R. Gonalez, Electrochim. Acta 47 (2002) 3715–3722.
[10] Q. Fan, C. Pu, E.S. Smotkin, J. Electrochem. Soc. 143 (1996) 3053–3057.
[11] W.-F. Lin, J.-T. Wang, R.F. Savinell, J. Electrochem. Soc. 144 (1997) 1917–1922.
[12] H. Houa, G. Suna, R. Heb, Z. Wu, B. Sun, J. Power Sources 182 (2008) 95–99.
[13] K. Bergamaski, E.R. Gonzalez, F.C. Nart, Electrochim. Acta 53 (2008) 4396–4406.
[14] E. Ribadeneira, B.A. Hoyos, J. Power Sources 180 (2008) 238–242.
[15] A. Ghumman, P.G. Pickup, J. Power Sources 179 (2008) 280–285.
[16] H. Songa, X. Qiu, D. Guob, F. Li, J. Power Sources 178 (2008) 97–102.
[17] Q. Wang, G.Q. Suna, L. Cao, L.H. Jiang, G.X. Wang, S.L. Wang, S.H. Yang, Q. Xin, J. Power Sources 177 (2008) 142–147.
[18] X. Xue, J. Ge, T. Tian, C. Liu, W. Xing, T. Lua, J. Power Sources 172 (2007) 560–569.
[19] M. Nie, H. Tang, Z. Wei, S.P. Jiang, P.K. Shen, Electrochem. Commun. 9 (2007) 2375–2379.
[20] E. Antolini, J. Power Sources 170 (2007) 1–12.
[21] H. Wang, C. Xu, F. Cheng, S. Jiang, Electrochem. Commun. 9 (2007) 1212–1216.
[22] R. Chetty, K. Scott, Electrochim. Acta 52 (2007) 4073–4081.
[23] A. Serov, C. Kwak, Appl. Catal. B: Environ. 91 (2009) 1–10.
[24] K.-D. Cai, G.-P. Yin, J. Zhang, Z.-B. Wang, C.-Y. Du, Y.-Z. Gao, Electrochem. Commun. 10 (2008) 238–241.
[25] J.-Y. Im, B.-S. Kim, H.-G. Choi, S.M. Cho, J. Power Sources 179 (2008) 301–304.
[26] S. Ueda, M. Eguchi, K. Uno, Y. Tsutsumi, N. Ogawa, Solid State Ionics 177 (2006) 2175–2178.
[27] M.M. Mench, H.M. Chance, C.Y. Wang, J. Electrochem. Soc. 151 (2004) A144–A150.
[28] Y. Liu, M. Muraoka, S. Mitsushima, K.-I. Ota, N. Kamiya, Electrochim. Acta 52 (2007) 5781–5788.
[29] L. Lu, G. Yin, Y. Tong, Y. Zhang, Y. Gao, M. Osawa, S. Ye, J. Electroanal. Chem. 619–620 (2008) 143–151.
[30] Y. Zhang, L. Lu, Y. Tong, M. Osawa, S. Ye, Electrochim. Acta 53 (2008) 6093–6103.
[31] J.-H. Yoo, H.-G. Choi, C.-H. Chung, S.M. Cho, J. Power Sources 163 (2006) 103–106.
[32] Y. Liu, S. Mitsushima, K. Ota, N. Kamiya, Electrochim. Acta 51 (2006) 6503–6509.
[33] J.-H. Yu, H.-G. Choi, S.M. Cho, Electrochem. Commun. 7 (2005) 1385–1388.
[34] G. Kerangueven, C. Coutanceau, E. Sibert, J.-M. Léger, C. Lamy, J. Power Sources 157 (2006) 318–324.
[35] Q. Zhang, Z. Li, S. Wang, W. Xing, R. Yu, X. Yu, Electrochim. Acta 53 (2008) 8298–8304.
[36] I. Mizutani, Y. Liu, S. Mitsushima, K. Ota, N. Kamiya, J. Power Sources 156 (2006) 183–189.
[37] A. Serov, C. Kwak, Appl. Catal. B: Environ. 90 (2009) 313–320.
[38] A.A. Serov, S.-Y. Cho, S. Han, M. Min, G. Chai, K.H. Nam, C. Kwak, Electrochem. Commun. 9 (2007) 2041–2044.
[39] A.A. Serov, M. Min, G. Chai, S. Han, S. Kang, C. Kwak, J. Power Sources 175 (2008) 175–182.
[40] A.A. Serov, C. Kwak, Catal. Commun. 10 (2009) 1551–1554.
[41] A.A. Serov, M. Min, G. Chai, S. Han, S.J. Seo, Y. Park, H. Kim, C. Kwak, J. Appl. Electrochem. 39 (2009) 1509–1516.
[42] A. Serov, T. Nedoseykina, O. Shvachko, C. Kwak, J. Power Sources 195 (2010) 175–180.
[43] E. Peled, V. Livshits, T. Duvdevani, J. Power Sources 106 (2002) 245–248.
[44] R.B. de Lima, V. Paganin, T. Iwasita, W. Vielstich, Electrochimi. Acta 49 (2003) 85–91.
[45] K. Matsuoka, Y. Iriyama, T. Abe, M. Matsuoka, Z. Ogumi, Electrochim. Acta 51 (2005) 1085–1090.
[46] A.O. Neto, T.R.R. Vasconselos, R.W.R.V. da Silva, M. Linardi, E.V. Spinacé, J. Appl. Electrochem. 35 (2005) 193–198.
[47] V. Livshits, E. Peled, J. Power Sources 161 (2006) 1187–1191.
[48] A.O. Neto, M. Linardi, E.V. Spinacé, Ionics 12 (2006) 309–313.
[49] T. Duvdevani, M. Philosoph, M. Rakhman, D. Golodnitsky, E. Peled, J. Power Sources 161 (2006) 1069–1075.
[50] R. Chetty, K. Scott, J. Appl. Electrochem. 37 (2007) 1077–1084.
[51] L. Demarconnay, S. Brimaud, C. Coutanceau, J.-M. Léger, J. Electroanal. Chem. 601 (2007) 169–180.
[52] S. Reichman, L. Burstein, E. Peled, J. Power Sources 179 (2008) 520–531.
[53] V. Livshits, M. Philosoph, E. Peled, J. Power Sources 178 (2008) 687–691.
[54] V. Selvaraj, M. Vinoba, M. Alagar, J. Colloid Interf. Sci. 322 (2008) 537–544.
[55] N. Travitsky, L. Burstein, Y. Rosenberg, E. Peled, J. Power Sources 194 (2009) 161–167.
[56] C. Jin, Y. Song, Z. Chen, Electrochimi. Acta 54 (2009) 4136–4140.
[57] R. Ojani, J.-B. Raoof, S. Fathi, Electrochimi. Acta 54 (2009) 2190–2196.
[58] Z.-P. Suna, X.-G. Zhang, Y.-Y. Liang, H.-L. Li, J. Power Sources 191 (2009) 366–370.
[59] N.W. Maxakato, C.J. Arendse, K.I. Ozoemena, Electrochem. Commun. 11 (2009) 534–537.
[60] F.J. Rodríguez Varela, S.F. Luna, R.D. Klapco, J. New Mater. Electrochem. Syst. 12 (2009) 003–008.
[61] H. Wang, Z. Jusys, R.J. Behm, Electrochim. Acta 54 (2009) 6484–6498.
[62] D. Morales-Acosta, L.G. Arriaga, L. Alvarez-Contreras, S. Fraire Luna, F.J. Rodríguez Varela, Electrochem. Commun. 11 (2009) 1414–1417.
[63] C. Lamy, E.M. Belgsir, in: W. Vielstich, A. Lamm, H.A. Gasteiger (Eds.), Handbook of Fuel Cells, vol. 1, Wiley, UK, 2003.
[64] P.A. Christensen, A. Hamnett, J. Electroanal. Chem. 260 (1989) 1101.
[65] F. Hahn, B. Beden, F. Kadirgan, C. Lamy, J. Electroanal. Chem. 216 (1987) 169.
[66] L.H. Leung, M.J. Weaver, J. Phys. Chem. 92 (1988) 4019.
[67] B. Wieland, J.P. Lancaster, C.S. Hoaglund, P. Holota, W.J. Tornquist, Langmuir 12 (1996) 2594.
[68] A. Daily, J. Shin, C. Korzeniewski, Electrochim. Acta 44 (1998) 1147.
[69] G. Horanyi, V.E. Kazarinov, Y.B. Vasil'ev, V.N. Andreev, J. Electroanal. Chem. 147 (1983) 263.
[70] C. Lamy, E.M. Belgsir, J.-M. Léger, J. Appl. Electrochem. 31 (2001) 799–809.
[71] H. Hoster, T. Iwasita, H. Baumgärtner, W. Vielstich, PCCP 3 (2001) 337.
[72] R. Chetty, K. Scott, J. New Mater. Electrochem. Syst. 10 (2007) 135.
[73] F. Kadirgan, B. Beden, C. Lamy, J. Electroanal. Chem. 136 (1982) 119.
[74] L.G.S. Pereira, F.R. dos Santos, M.E. Pereira, V.A. Paganin, E.A. Ticianelli, Electrochim. Acta 51 (2006) 4061.
[75] E.V. Spinacé, A.O. Neto, T.R.R. Vasconcelos, M. Linardi, Brazilian Patent INPI-RJ, PI0304121-2, 2003.
[76] E.V. Spinacé, A.O. Neto, T.R.R. Vasconcelos, M. Linardi, J. Power Sources 137 (2004) 17.
[77] N. Travitsky, T. Ripenbein, D. Golodnitsky, Y. Rosenberg, L. Burshtein, E. Peled, J. Power Sources 161 (2006) 782.
[78] M. Philosoph, Ph.D. Thesis, Tel Aviv University, November 2008.
[79] E. Antolini, T. Lopes, E.R. Gonzalez, J. Alloys Compd. 461 (2008) 253.
[80] E. Peled, T. Duvdevani, A. Melman, Eletrochem. Solid-State Lett. 1 (5) (1998) 210.
[81] E. Peled, T. Duvdevani, A. Aharon, A. Melman, Electrochem. Solid-State Lett. 4 (4) (2001) A38–A41.
[82] J. Solla-Gullon, A. Rodes, V. Montiel, A. Aldaz, J. Clavillier, J. Electroanal. Chem. 554–555 (2003) 273.